Radiation Protection Dosimetry (2010), pp. 1–7 doi:10.1093/rpd/ncq493

# FEASIBILITY STUDY ON USING IMAGING PLATES TO ESTIMATE THERMAL NEUTRON FLUENCE IN NEUTRON-GAMMA MIXED FIELDS

Toshioh Fujibuchi[1,2,*], Yu Tanabe[1], Takeji Sakae[1,3], Toshiyuki Terunuma[1,3], Tomonori Isobe[1,3], Hiraku Kawamura[1,2], Kiyoshi Yasuoka[1,3], Tetsuro Matsumoto[4], Hideki Harano[4], Jun Nishiyama[4], Akihiko Masuda[4] and Akihiro Nohtomi[5]

[1]Graduated School of Comprehensive Human Sciences, University of Tsukuba, 1-1-1 Tennodai, Tsukuba, Ibaraki 305-8575, Japan

[2]School of Health Science, Ibaraki Prefectural University of Health Sciences, 4669-2 Ami, Ami-machi, Inashiki-gun, Ibaraki 300-0394, Japan

[3]Proton Medical Research Center, University of Tsukuba, 1-1-1 Tennodai, Tsukuba, Ibaraki 305-8575, Japan

[4]Quantum Radiation Division, National Metrology Institute of Japan, National Institute of Advanced Industrial Science and Technology, 1-1-1 Umezono, Tsukuba, Ibaraki 305-8568, Japan

[5]Atomic Energy Research Institute, Kinki University, 3-4-1 Kowakae, Higashiosaka-shi, Osaka 577-8502, Japan

*Corresponding author: fujibuchi@ipu.ac.jp

*Received April 19 2010, revised November 8 2010, accepted November 25 2010*

**In current radiotherapy, neutrons are produced in a photonuclear reaction when incident photon energy is higher than the threshold. In the present study, a method of discriminating the neutron component was investigated using an imaging plate (IP) in the neutron–gamma-ray mixed field. Two types of IP were used: a conventional IP for beta- and gamma rays, and an IP doped with Gd for detecting neutrons. IPs were irradiated in the mixed field, and the photo-stimulated luminescence (PSL) intensity of the thermal neutron component was discriminated using an expression proposed herein. The PSL intensity of the thermal neutron component was proportional to thermal neutron fluence. When additional irradiation of photons was added to constant neutron irradiation, the PSL intensity of the thermal neutron component was not affected. The uncertainty of PSL intensities was approximately 11.4 %. This method provides a simple and effective means of discriminating the neutron component in a mixed field.**

## INTRODUCTION

In the evaluation of irradiation characteristics for neutron capture therapy, which is a modality that principally destroys cancers selectively at the cellular level, it is important to measure the distribution of the neutron flux[1]. In proton therapy, neutrons are also produced by (p,n) reactions[2, 3]. Fast neutrons are thermalised by hydrogen in the patient's body, and thermal neutrons are produced. Thermal neutrons cause software errors in pacemakers and other medical devices, as well as radioactivation in the treatment room[4]. Therefore, the evaluation of neutrons is of importance in medical fields.

Neutron dosimetry is generally performed by activation methods[5, 6], CR-39[2, 7, 8], bubble detectors[1] or Bonner sphere spectrometry.[5] However, the analyses involved in these methods are complex. Imaging plates (IPs) use a photostimulable phosphor of $BaFBr:Eu^{2+}$ and are currently used in numerous fields, including medicine, bioscience and physics[8–13]. Latent images on the IP that are created by ionising radiation are scanned by a stimulating laser beam and are read by a photomultiplier as photo-stimulated luminescence (PSL).

In the present study, a thermal neutron detector was constructed using IPs and Cd plates, and investigated a method for discriminating the PSL intensity of the thermal neutron component in a neutron–gamma-ray mixed field. The basic characteristics of this method and its accuracy in discriminating PSL intensity were verified. In radiotherapy field, the evaluation of the neutron energy is difficult. Therefore, thermal neutron standard field in the feasibility study was used.

## MATERIALS AND METHODS

### Imaging plates

Two types of IP was used: a conventional IP (BAS-MS 2025, Fuji Photo Film Co., Ltd., Tokyo, Japan) for beta- and gamma rays and another IP (BAS-ND 2025, Fuji Photo Film Co., Ltd.) for detecting

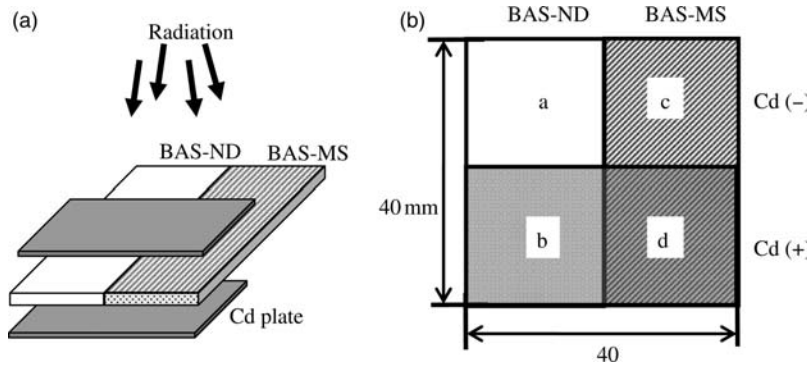


Figure 1. Configuration of the neutron detector: (**a**) structure and (**b**) top view.

neutrons[12]. BAS-ND is sensitised by $Gd_2O_3$ converter molecules, which efficiently absorb neutrons. Nuclear reactions of Gd with neutrons produce gamma rays of 0.3, 0.4, 1.2 MeV and other energies, and internal conversion electrons with an average energy of approximately 70 keV. These excite photostimulable BaFBr:$Eu^{2+}$ phosphor molecules that are dispersed in the phosphor layer[14].

After irradiation, the PSL intensities were read and analysed using an image scanner (FLA7000, Fuji Photo Film Co., Ltd.) and its dedicated software (Image Gauge, Fuji Photo Film Co., Ltd.). The fixed scanning parameters were as follows: latitude, 5; sensitivity, 10 000; and resolution, 100 μm.

### Neutron detector and discrimination of the neutron component

Since the BAS-ND is sensitive to other radiation as well as neutrons, it is necessary to discriminate the components of other radiation. The following method was investigated.

A part of the BAS-ND IP was covered with a Cd plate (thickness, 1.0 mm[15]) on the upper and lower surfaces. The difference in the PSL intensity of the BAS-ND with or without Cd to be primarily due to thermal neutrons was considered. However, since a certain quantity of gamma rays from the radiation source is absorbed by the upper Cd filter, prompt gamma rays from the Cd plate are also detected. In order to eliminate the effect of gamma rays, a part of the BAS-MS was also covered with a Cd plate on the upper and lower surfaces, as shown in Figure 1. Thus, the detector was divided into four regions: (a) BAS-ND without Cd, (b) BAS-ND with Cd, (c) BAS-MS without Cd, and (d) BAS-MS with Cd. During irradiation, the IP was covered with a light-proof sheet of radiographic film (thickness: 0.1 mm) on the front and a black acrylic envelope (thickness: 2.0 mm) on the reverse to exclude room light.

The PSL intensities for each region represent the following radiation component:

$$\mathrm{a} : N_{\mathrm{Gd}} + N_{\mathrm{Eu,BAS-ND}} + \gamma_{\mathrm{source}}, \quad (1)$$

$$\mathrm{b} : \gamma_{\mathrm{source}} \times A + \gamma_{\mathrm{Cd}}, \quad (2)$$

$$\mathrm{c} : (\gamma_{\mathrm{source}} + N_{\mathrm{Eu,BAS-MS}}) \times R_{\mathrm{MS/ND}}, \quad (3)$$

$$\mathrm{d} : (\gamma_{\mathrm{source}} \times A + \gamma_{\mathrm{Cd}}) \times R_{\mathrm{MS/ND}}, \quad (4)$$

where $N_{\mathrm{Gd}}$ is the thermal neutron component of Gd in BAS-ND, $N_{\mathrm{Eu}}$ is the thermal neutron component of Eu in BAS-ND and BAS-MS, $\gamma_{\mathrm{source}}$ is radiation (e.g. photons, electrons, and other particle radiation) other than thermal neutrons from the source, $\gamma_{\mathrm{Cd}}$ is prompt gamma rays from Cd, $A$ is the attenuation factor for Cd (including absorption and scattering of radiation) and $R_{\mathrm{MS/ND}}$ is the response ratio of the BAS-MS to BAS-ND.

The IP uses electrons from the ionisation $Eu^{2+}$ to $Eu^{3+}$ in making signals. Neutron irradiation induces the $^{151}Eu(n,\gamma)^{152}Eu$ and $^{153}Eu(n,\gamma)^{154}Eu$ reactions[11], which may cause ionisation and produce the signal for the BAS-ND and BAS-MS. The contribution of these reactions to the IP signal is estimated assuming that one reaction produces one signal, although this assumption may lead to overestimation. In order to estimate the signals produced by these reactions, the atomic density $N$ and cross-sectional $\sigma_{\mathrm{th}}$ for thermal neutrons are listed in Table 1. The rate of the nuclear reaction is roughly proportional to $N\sigma_{\mathrm{th}}$. The value of $N\sigma_{\mathrm{th}}$ for $^{157}Gd(n,\gamma)^{158}Gd$ is three orders of magnitude higher than that for $^{151}Eu(n,\gamma)^{152}Eu$ and is five orders of magnitude higher than that for $^{153}Eu(n,\gamma)^{154}Eu$. Therefore, the value of $N_{\mathrm{Eu}}$ to be nearly equal 0 was selected. Although this is correct in most cases, the actual value of $N_{\mathrm{Eu}}$ is dependent on the n/γ ratio. If this ratio is very high, then this value of $N_{\mathrm{Eu}}$ might not be appropriate. However, in the high n/γ ratio

**Table 1. Rate of Gd and Eu cross sections.**

| | Reaction | Planar density of target atom $N$ in the IP (atom cm$^{-2}$) | Cross section for thermal neutron $\sigma_{th}$ (barn=$10^{-24}$ cm$^2$) | $N\sigma_{th}$ (atom) |
|---|---|---|---|---|
| BAS-ND | $^{157}$Gd(n,g)$^{158}$Gd | $1.0 \times 10^{19}$ | $2.5 \times 10^{5}$ | 2.6 |
| | $^{151}$Eu(n,g)$^{152}$Eu | $1.5 \times 10^{17}$ | $9.2 \times 10^{3}$ | $1.4 \times 10^{-3}$ |
| | $^{153}$Eu(n,g)$^{154}$Eu | $1.6 \times 10^{17}$ | $3.9 \times 10^{2}$ | $6.3 \times 10^{-5}$ |
| BAS-MS | $^{151}$Eu(n,g)$^{152}$Eu | $5.3 \times 10^{17}$ | $9.2 \times 10^{3}$ | $4.9 \times 10^{-3}$ |
| | $^{153}$Eu(n,g)$^{154}$Eu | $5.6 \times 10^{17}$ | $3.9 \times 10^{2}$ | $2.2 \times 10^{-4}$ |

field, $N_{Eu,\ BAS\text{-}MS}$ in Equation (3) increases, but $N_{Eu,\ BAS\text{-}ND}$ in Equation (1) also increases. Therefore, $N_{Eu,\ BAS\text{-}MS}$ and $N_{Eu,\ BAS\text{-}ND}$ are counterbalanced in Equation (7) ($=N_{Gd}$) and do not affect greatly.

From Equations (1) through (4), the following equations have been obtained:

$$R_{MS/ND} = \frac{d}{b}, \tag{5}$$

$$\gamma_{source} = \frac{c}{R_{MS/ND}} = \frac{bc}{d}, \tag{6}$$

$$N_{Gd} = a - \gamma_{source} = a - \frac{bc}{d}. \tag{7}$$

Thus, the thermal neutrons and other radiation components can be discriminated.

### Fading characteristics

The latent image of radiation stored in an IP fades with time, a phenomenon referred to as fading[9, 12]. Fading is an important characteristic of dosimetry using IPs. Fading depends on the type of IP, the annealing temperature, and the image reader, but not on the type of radiation[16]. The fading characteristics up to 72 h after irradiation for a 6-MV photon beam (0.025 Gy) at 25°C was measured.

### Evaluation of the characteristics about IPs in a neutron–gamma-ray mixed field

In order to evaluate the accuracy of the present investigative method, the thermal neutron standard field of the National Institute of Advanced Industrial Science and Technology, Japan was used. The thermal neutron field was established outside of a graphite pile (rectangular dimensions: 190 cm × 190 cm × 230 cm) with an Am-Be neutron source (148 GBq). The detectors were placed at a distance of 40 cm from the surface of the graphite pile and were irradiated for 2, 4, 6, 8, and 67 h. The experimental setup is shown in Figure 2. The thermal neutron fluence rate in the corresponding area for the IP was measured using a $^3$He spherical proportional counter (SP9: Centronic Ltd., Croydon, UK). The IPs were also exposed (after 67 h of moderated Am-Be irradiation) to 6-MV photons of 2 or 4 mGy in order to verify the validity of Equations (5) through (7) for discriminating neutrons and photons.

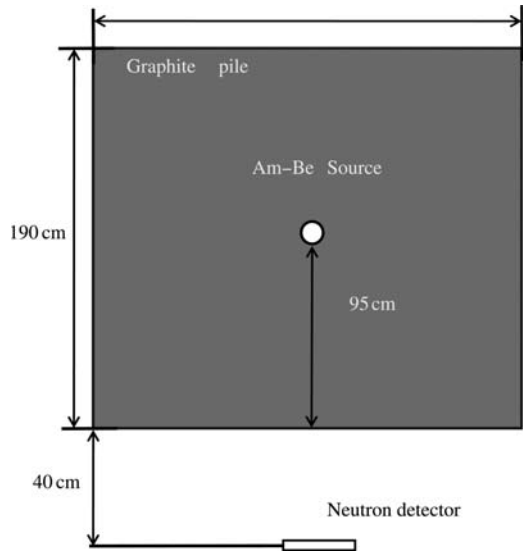


Figure 2. Set-up for the measurement of linearity of IPs in a graphite pile (top view; size: 190 × 190 × 230 cm).

## RESULTS AND DISCUSSION

### Fading characteristics

The estimations of 6-MV photon irradiation by BAS-MS and BAS-ND are shown in Figure 3. The curves were normalised by PSL intensity per photon dose at the termination of irradiation ($t$=0 h, $I_0$(PSL mm$^{-2}$ Gy$^{-1}$)). Each experimental data set can be well fitted by a combination of two exponential curves with different time constants. The results of data fitting with two exponential decay functions

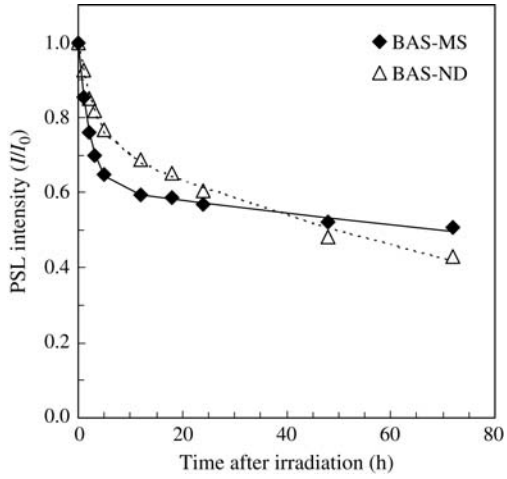


Figure 3. Normalised fading curves of PSL intensity.

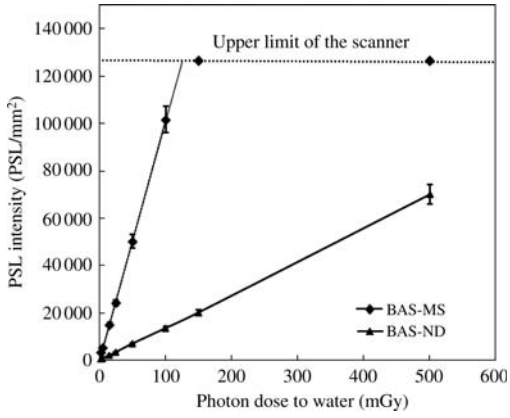


Figure 4. Linearity of PSL intensities for BAS-MS and BAS-ND to a photon dose of 6 MV.

yield the following equations:

$$\frac{I(t)}{I_{0,\mathrm{BAS-MS}}} = 0.39\ \exp(-0.46t) + 0.61\ \exp(-0.0029t), \quad (8)$$

$$\frac{I(t)}{I_{0,\mathrm{BAS-ND}}} = 0.26\ \exp(-0.35t) + 0.74\ \exp(-0.0082t). \quad (9)$$

The experimental uncertainty for the PSL intensity of BAS-MS was 1.4 % and that of BAS-ND was 0.9 % as a result of four measurements under each time condition.

This value was used as the relative error of the experimental results using the IP.

### Fading correction of PSL intensity

The PSL intensities of the IPs irradiated with the graphite pile were corrected to eliminate fading during irradiation and after the termination of irradiation, as follows:

$$\begin{aligned} I(t) &= I_0 \div t_i \times \int_{t_f}^{t_i+t_f} (\alpha \cdot \exp(-\lambda_1 t) + \beta \cdot \exp(-\lambda_2 t))\mathrm{d}t \\ &= I_0 \div t_i \times \left[ \left(-\frac{\alpha}{\lambda_1}\exp(-\lambda_1 t) - \frac{\beta}{\lambda_2}\exp(-\lambda_2 t)\right)\right]_{t_f}^{t_i+t_f} \\ &= I_0 \div t_i \times \left(\frac{\alpha}{\lambda_1}(\exp(-\lambda_1 t_f) - \exp(-\lambda_1(t_i+t_f)))\right) \\ &\quad + \left(\frac{\beta}{\lambda_2}(\exp(-\lambda_2 t_f) - \exp(-\lambda_2(t_i+t_f)))\right) \end{aligned}, \quad (10)$$

where $t_i$ is the irradiation time, $t_f$ is the fading time from the termination of irradiation to IP readout, alpha and beta are the ratios of the two exponential decay functions, and $\lambda_1$ and $\lambda_2$ are the decay components of the fading curve derived by Equations (8) and (9), respectively.

### Linearity of the PSL intensity during photon and thermal neutron exposure

The relationship between the PSL intensities of BAS-MS and BAS-ND to the 6-MV photon dose in water is shown in Figure 4.

Assuming a Poisson distribution, the counting value and the counting error can be expressed by following equation:

$$\frac{x}{A} \pm \frac{\sqrt{x}}{A}, \quad (11)$$

where $x$ is the value of the PSL, $A$ is the readout area ($\mathrm{mm}^2$) and $x/A$ is the PSL intensity (PSL $\mathrm{mm}^{-2}$). Since the IP is a two-dimensional detector, the value of $A$ is required in Equation 11.

The ratio of the counting error to the counting value can be evaluated by the following equation:

$$E = \frac{\sqrt{x}/A}{x/A}. \quad (12)$$

Since the readout area is fixed at 100 $\mathrm{mm}^2$ in the experiment, the value of $x$ is calculated as 1 PSL $\mathrm{mm}^{-2}$ if a 10 % error is allowed ($E$=0.1 in Equation 12).

The PSL intensities of the BAS-MS were proportional to the photon dose up to at least 100 mGy. Above 150 mGy, there was no change in the PSL intensity beyond 126 468 PSL $mm^{-2}$, which is the upper limit of the scanner's range. This value is a specification of the scanner. PSL of this scanner has the width of five digits. The PSL intensities of the BAS-ND exhibited proportionality to at least 500 mGy.

The linearity of the PSL intensities of the IPs with fading correction to neutron fluence as calculated using Equations (5) through (7) and Equation (10) in the moderated Am-Be field is shown in Figure 5. The neutron fluence rate measured by the proportional counter was $6.72 \times 10^{1}$ $cm^{-2}$ $s^{-1}$. Therefore, the irradiated neutron fluence rates were $4.8 \times 10^{5}$, $9.7 \times 10^{5}$, $1.5 \times 10^{6}$, $1.9 \times 10^{6}$ and $1.6 \times 10^{7}$ $cm^{-2}$, under the conditions shown in Figure 2. In ICRP publication 74, the fluence-to-dose equivalent $H^*(10)$ conversion factor for neutrons ($1.00 \times 10^{-9}$ MeV) is 6.9 pSv $cm^2$[17]. Thus, the following dose equivalents are obtained: 3.4, 6.7, 10.0, 13.4 and 112.5 μSv. The PSL intensities were proportional to the neutron fluence.

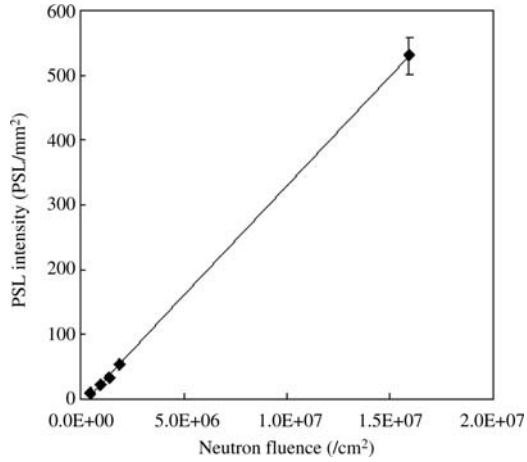


Figure 5. Linearity of PSL intensity with fading correction with respect to neutron fluence in the moderated Am-Be field.

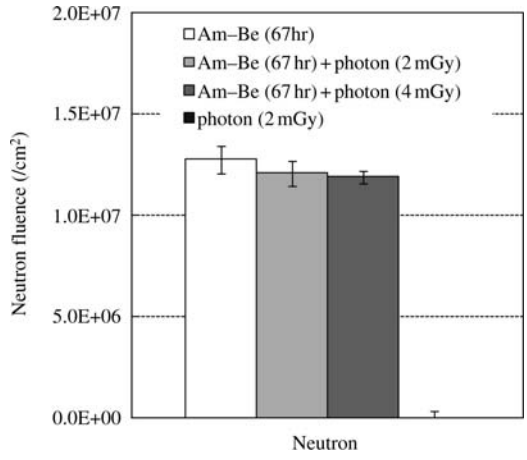


Figure 6. Neutron fluence of an IP irradiated in the neutron–gamma-ray mixed field.

## Characterisation of IPs in a neutron–gamma-ray mixed field

The PSL intensities of the IPs irradiated in the neutron–gamma-ray mixed field with 6-MV boost photons were corrected for fading using Equation (10), and neutrons and photons were discriminated using Equations (5) through (7). Figure 6 converts the PSL intensities to neutron fluence in a mixed field using the results of Figures 4 and 5. In a student's *t*-test, the *p* value between moderated Am-Be (67 h) and moderated Am-Be (67 h)+photon 2 mGy was 0.019 and that between moderated Am-Be (67 h) and moderated Am-Be (67 h)+photon 4 mGy was 0.003. The values of neutron fluence were similar with and without additional photon irradiation. The combined uncertainty of the PSL intensity of the BAS-MS and BAS-ND was 11.4 %. This uncertainty evaluated from eight times measurement, and contains the influence of the fading, energy dependence, reproducibility. Accordingly, it was confirmed that the neutron component could be discriminated precisely in a neutron–gamma-ray mixed field.

Figure 4 indicates that the response to photons is approximately 100 PSL $cm^{-2}$ $mGy^{-1}$ for the BAS-ND. From Figure 5 and the conversion factor of the ICRP, the response to neutrons is approximately 20 000 PSL $cm^{-2}$ $mSv^{-1}$. If the standard deviation of the photon signal is larger than that of the neutron signal, then the neutron signal may obscure the photon signal. Therefore, if the γ/n dose ratio exceeds 2000, the proposed method may fail.

## Advantage of the IP discrimination method

Using the characteristics of the IP, the proposed method can measure a small amount of thermal neutron fluence with a wide dynamic range and high sensitivity.

The neutron particle fluence that can be detected is on the order of $10^{5}$ $cm^{-2}$ $s^{-1}$, because the minimum value of PSL that can be read is approximately 1. The IP has the advantage of re-usability for radiation measurement. Since the sensitivity of the IP is energy dependent for photon detection, a correction factor should be estimated in the measurements[11]. Furthermore, the energy response differs depending on the type of IP used[9, 11]. The

energy response of IPs depends on the composition of photostimulable high-Z phosphor material and thickness. It is necessary to consider these corrections in measurements obtained using different types of IPs and to use a correction factor in the present method because the energy dependence is always measured as the response ratio $R_{MS/ND}$. In the present study, $R_{MS/ND}$ was $7.65 \pm 0.79$ in the 6-MV photon beam field, and $9.43 \pm 0.89$ in the neutron–gamma-ray mixed field.

### Points to consider when using the proposed method

The fading curves differed with the type of IP (Figure 3). Fading must be taken into consideration because $R_{MS/ND}$ changes as a function of fading time. Decay by fading is fast, and occurs immediately after irradiation. Therefore, reading should be delayed by several hours in order to reduce the margin of error in the fading correction. Furthermore, fading curves are sensitive to temperature[9]. Therefore, it is necessary to manage the IP temperature when performing measurements with fading.

In the case of excessive amounts of photons in the measurement field, the PSL intensity of the BAS-MS may be saturated. Furthermore, when the PSL intensity of the photon component greatly exceeds that of the neutron component, the neutron component may be obscured by fluctuations in the photon component. Therefore, the amount of radiation and the ratio of photons to neutrons in the measurement field must be controlled.

### Future considerations

The BAS-ND enables detection of neutrons when Gd is included in the phosphor layer. Gd has a large cross section for thermal neutron interactions, whereas the cross section for fast neutrons is very small. In the proposed method, the accuracy to detect thermal neutrons can be improved using a Cd shielding. Fast neutrons that penetrate Cd were not considered in the present study. In the neutron field formed using the graphite pile, thermal neutrons predominated, and thus the influence of fast neutrons can largely be disregarded. The cadmium ratio is approximately 100 at 90 cm from the centre of the moderated Am-Be[14]. In order to estimate a field in which fast neutrons are more abundant, the fast neutron component must be taken into consideration. By arranging a charged particle converter in front of the neutron detector[8], fast neutrons should be considered in mixed field measurements in future studies.

## CONCLUSIONS

In the present study, a method of measuring thermal neutrons in a neutron–gamma-ray mixed field was developed using IPs. Using two types of IPs and a Cd plate, discrimination of the thermal neutron component with an uncertainty of 11.4 % was confirmed. The IP has fading characteristics and its sensitivity is energy dependent. Taking these characteristics into consideration, the newly developed method is suggested to be able to measure the thermal neutron.

## REFERENCES


1. Wang, C. K., Blue, T. E. and Gahbauer, R. *Neutronic study of an accelerator-based neutron irradiation facility for Boron neutron capture therapy.* Nucl. Technol. **84**, 93–107 (1989).
2. Moyers, M. F., Benton, E. R., Ghebremedhin, A. and Coutrakon, G. *Leakage and scatter radiation from a double scattering based proton beamline.* Med. Phys. **35**, 128–144 (2008).
3. Hall, E. J. *Intensity-modulated radiation therapy, protons, and the risk of second cancers.* Int. J. Radiat. Oncol. Biol. Phys. **65**, 1–7 (2006).
4. Kim, H. S., Park, Y. H., Koo, B. C., Kwon, J. W., Lee, J. S. and Choi, H. S. *Evaluation of the photoneutron field produced in a medical linear accelerator.* Radiat. Prot. Dosim. **123**, 323–328 (2007).
5. Fernandez, F., Domingo, C., Amgarou, K., Castelo, J., Bouassoule, T., Gareia, M. J. and Luguera, E. *Neutron measurement in a varian 2100C linac facility using bonner sphere system based on passive gold activation detectors.* Radiat. Prot. Dosim. **126**, 361–365 (2007).
6. Fujibuchi, T., Yamaguchi, I., Kasahara, T., Iimori, T., Masuda, Y., Kimura, K., Watanabe, H., Isobe, T. and Sakae, T. *Measurement of thermal neutron fluence distribution with use of $^{23}$Na radioactivation around a medical compact cyclotron.* Radiol. Phys. Technol. **2**, 159–165 (2009).
7. Benton, E. V., Ogura, K., Frank, A. L., Atallah, T. and Rowe, V. *Response of different types of CR-39 to energetic ions.* Nucl. Tracks Radiat. Meas. **12**, 79–82 (1986).
8. Belafrites, A., Nourreddine, A., Mouhssine, D., Nachab, A., Pape, A., Boucenna, A. and FernaAndez, F. *Comparison of imaging plates with track detectors for fast-neutron dosimetry.* Radiat. Prot. Dosim. **110**, 333–336 (2004).
9. Ohuchi, H., Yamadera, A. and Baba, M. *Development of a new passive integral dosemeter for gamma ray monitoring using imaging plate.* Radiat. Prot. Dosim. **107**, 239–246 (2003).
10. Olch, J. *Evaluation of a computed radiography system for megavoltage photon beam dosimetry.* Med. Phys. **32**, 2987–2999 (2005).
11. Tanaka, K., Endo, S. and Hoshi, M. *Measurements of neutron distribution in neutrons—γ-rays mixed field using imaging plate for neutron capture therapy.* Appl. Radiat. Isot. **68**, 207–210 (2010).
12. Karasawa, Y., Kumazawa, S. and Niimura, N. *The character and application of a neutron imaging plate.* Phys. B **241–243**, 139–141 (1998).
13. Suzuki, T., Mori, C., Yanagida, K., Uritani, A., Miyahara, H., Yoshida, M. and Takahashi, F. *Characteristics and correction of the Fading of imaging plate.* J. Nucl. Sci. Technol. **34**, 461–465 (1997).

14. Takahashi, K., Tazaki, S., Miyahara, J., Karasawa, Y. and Niimura, N. *Imaging performance of imaging plate neutron detectors.* Nucl. Instrum. Methods Phys. Res. A **377**, 119–122 (1996).
15. Harano, H., Matsumoto, T., Shimoyama, T., Sato, Y., Uritani, A., Hino, Y., Kudo, K. and Michikawa, T. *Convenient method of relative calibration of the neutron source emission rate between different source type.* IEEE Trans. Nucl. Sci. **53**, 1413–1417 (2006).
16. Ohuchi, H. and Yamadera, A. *Dependence of fading patterns of photo-stumulated luminescence from imaging plates of radiation, energy, and image reader.* Nucl.Instrum. Methods **A490**, 573–582 (2002).
17. Veinot, K. G. and Hertel, N. E. *Effective quality factors for neutrons based on the revised ICRP/ICRU recommendations.* Radiat. Prot. Dosim. **115**, 536–541 (2005).